SMAR 2015 – Third Conference on Smart Monitoring,
Assessment and Rehabilitation of Civil Structures

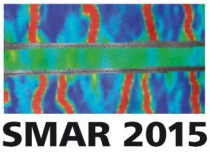


# Fatigue performance of RC beams strengthened in shear with externally bonded CFRP sheets: An experimental study on the effect of cyclic loading

Georges El-Saikaly[1], and Omar Chaallal[2]

[1] PhD candidate, Dept. of Construction Engineering, University of Quebec, École de Technologie Supérieure, Montréal QC, Canada H3C 1K3. E-mail: georges.el-saikaly.1@ens.etsmtl.ca
[2] Full professor, Dept. of Construction Engineering, University of Quebec, École de Technologie Supérieure, Montréal QC, Canada H3C 1K3. E-mail: omar.chaallal@etsmtl.ca

ABSTRACT: Studies on the behavior of beams retrofitted under fatigue loading are relatively few, particularly in shear. This study examined the fatigue performance of six RC T-beams retrofitted in shear using EB-CFRP sheets. Two cyclic loading options and three transverse steel ratios were considered. The results confirmed the feasibility of using the EB-FRP technique in extending the service life of beams. It also confirmed that the presence of stirrups enhance the fatigue performance of beams.

## 1 INTRODUCTION

RC bridge girders are usually subjected to cyclic loadings below their static capacities, which may increase the rate of damage due to cumulative fatigue degradation. The use of externally bonded (EB) fiber-reinforced polymer (FRP) for rehabilitation or strengthening of deficient structures is gaining worldwide popularity. Strengthening with FRP under static loading is well documented in both flexure and shear. However, experimental research studies involving long-term cycling loading (fatigue) are limited, especially those dealing with RC members retrofitted in shear (Czaderski and Motavalli 2004; Williams and Higgins 2008; Chaallal et al. 2010; Bae et al. 2013). The study presented in this paper aimed to examine experimentally the fatigue performance of RC T-beams strengthened in shear using EB-CFRP sheets. It considered two different applied cyclic loadings related to two practical objectives: (i) strengthen the RC beam to upgrade its shear capacity (category-U); and (ii) retrofit the deficient beam to match its original shear capacity (category-R). The test results are presented in terms of modes of failure, stiffness degradation, deflection response, and strain responses undergone by steel reinforcement (longitudinal and transverse) and CFRP. The effectiveness of the EB-FRP technique in extending the service life and enhancing the fatigue behavior of RC beams retrofitted in shear is discussed.

## 2 EXPERIMENTAL PROGRAM

### *2.1 Test specimens and properties of materials*

Six laboratory tests were performed on RC T-beams, with 4520 mm total length and 406 mm total depth. Details of specimens are illustrated in Figure 1. The yield stress, $f_y$, achieved by the

25M and 8M bars were 470 MPa and 640 MPa, respectively. The 28-day concrete compression strength, $f'_c$, was 35 MPa on average. The composite material used in this investigation was a unidirectional carbon-fiber fabric applied continuously in one ply over the test zone in a U shape using a wet lay-up procedure. The CFRP sheets were characterized, as reported by the manufacturer, by an ultimate tensile strength of 894 MPa, elastic modulus of 65 GPa, elongation at rupture of 1.33%, and a thickness of 0.381 mm for cured laminate sheet impregnated with epoxy resin. The designation of test specimens is presented in Table 1 for both U- and R-categories. Three series (S0, S1 and S3) of internal transverse steel reinforcement are considered.

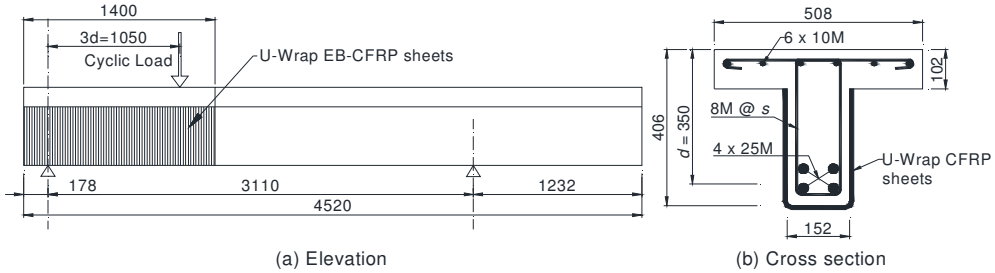


Figure 1. Details of test specimens.

Table 1. Test specimens designation

| | Series S0 (no stirrups) | Series S1 ($s = d/2$) | Series S3 ($s = 3d/4$) |
|---|---|---|---|
| Category-U | S0-U | S1-U | S3-U |
| Category-R | S0-R | S1-R | S3-R |

### *2.2 Test setup and instrumentation*

The T-beam specimens were tested in three-point load bending and subjected to fatigue loading up to 6 million cyclic loads at a rate of 3 Hz. The specimens that did not fail under fatigue were then tested under static loading up to failure. The fatigue load was cycled from 35% to 65% of the load carrying capacity $P$ of beams, where $P$ depended on the category. For both categories, the ultimate loads at rupture $P$ were obtained from similar specimens previously tested under static loading. Table 2 presents the loading conditions for each specimen. For static loading, the tests were performed under displacement control conditions at a rate of 2 mm/min. The lower and upper limits of cyclic loads, $P_{min}$ and $P_{max}$, evolve with respect to a mean value estimated at 50% of ultimate, corresponding to the passage of a standard vehicle at a crawling speed. The test setup and instrumentation of gauges are shown in Figure 2. The vertical displacement was measured under the point of applied load. The longitudinal-steel was instrumented with a strain gauge under the applied load. Strain gauges were affixed to the stirrups located in the loading zone along the expected plane of shear failure. The deformations experienced by the CFRP sheets were measured using crack gauges. These gauges were installed vertically onto the lateral faces at the same positions as the internal stirrup strain gauges.

Table 2. Cyclic loading conditions

| Specimen | Ultimate static load, $P$ (kN) | Applied cyclic loads | | |
|---|---|---|---|---|
| | | $P_{max}$ (65%) | $P_{min}$ (35%) | Load range (30%) |
| S0-U | 196 | 127 | 69 | 58 |
| S1-U | 393 | 255 | 137 | 118 |
| S3-U | 335 | 218 | 118 | 100 |
| S0-R | 137 | 89 | 49 | 40 |
| S1-R | 365 | 237 | 127 | 110 |
| S3-R | 294 | 191 | 103 | 88 |

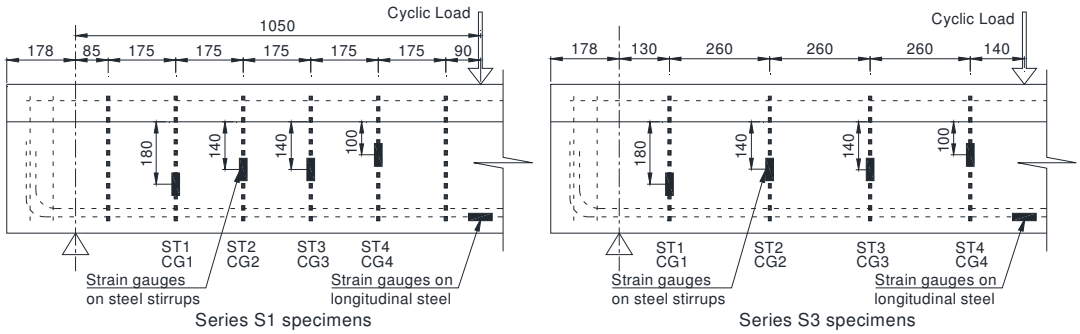


Figure 2. Test setup and instrumentation of gauges.

## 3 TEST RESULTS

All test specimens exhibited an accelerated damage accumulation characterized by an initial increase in the deflection response and the strains in internal steel reinforcement and EB-FRP during the early cycles, followed by a stable phase in which the rate of damage progressed gradually during the fatigue loading. This stable phase extended up to the last, very short phase just before imminent failure, which was characterized by a sudden increase in deflection and strain before failure.

### *3.1 Failure modes*

The failure modes at rupture of test specimens under fatigue and static (post-fatigue) loading, as well as the rupture of steel reinforcement after removal of concrete are shown in Figure 3. For category-U specimens, the two specimens with internal stirrups failed in flexure fatigue (Figure 3(a,b)). However, both specimens endured more than 5 million cycles. No yielding or rupture of steel-stirrups was observed in these specimens before flexure fatigue failure. Specimen S0-U, which did not fail in fatigue, failed in shear under static loading. All specimens of category-R endured more than 6 million cycles without any fatigue failure. No yielding of the internal steel reinforcement (longitudinal and transverse) was observed in these specimens during the whole course of fatigue tests. They were failed in shear under static loading (Figure 3(c,d)). In terms of fatigue life, category-R specimens (which did not fail in fatigue) showed an enhanced extension in comparison with category-U specimens (which failed before 6 million cycles). Nevertheless, despite their flexure fatigue failure, the latter specimens resisted more than 5 million cycles at very high stress range, demonstrating the efficiency and the potential of the EB-FRP shear strengthening technique to enhance the fatigue behavior of existing RC structures. However, in

RC beams strengthened to upgrade the service load, the longitudinal steel may be the weakest link, especially for extended service life in which case it may govern the upper limit of the projected capacity.

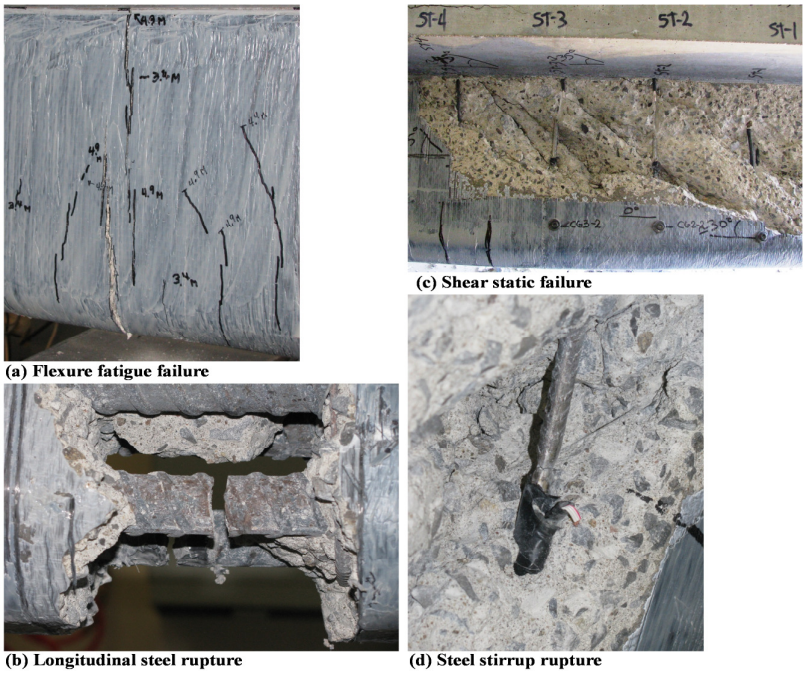


(a) Flexure fatigue failure

(c) Shear static failure

(b) Longitudinal steel rupture

(d) Steel stirrup rupture

Figure 3. Failure modes under fatigue and static loading.

### *3.2 Deflection response*

Figure 4(a) presents the variation of the deflection response for the maximum applied load ($P_{max}$) with increasing number of cycles. For specimens S1-U and S3-U that failed in flexure fatigue, their deflection response exhibited a sudden increase due to steel yielding before failure. It can be observed that category-R specimens, i.e., with no increase in service load, behaved extremely well and outperformed those strengthened for increased service load. This can be attributed to the fact that specimens of category-U were subjected to higher applied cyclic load ranges.

### *3.3 Strain responses*

#### 3.3.1 Transverse steel

Figure 4(b) shows the curves representing the maximum strains in the transverse steel versus the number of cycles. For both categories, the stirrup strains increased as the spacing decreased due to the increased capacity and hence the applied fatigue loading. However, a comparison between the series S1 (spaced at $d/2$) and S3 (spaced at $3d/4$) revealed an enhanced fatigue performance of the transverse steel for S1 specimens, even if they were subjected to a higher level of stress range. Therefore, the retrofitted specimens exhibited a more ductile behavior with the increase in the amount of transverse steel reinforcement.

The maximum strain recorded in S1-U (1860 $\mu\varepsilon$) at failure represented 56% of the yield stress, whereas that of S1-R at 6 million cycles (2160 $\mu\varepsilon$) represented 65%. For comparison, the ACI 440.2R-08 guideline states, in this context, that the stress in the longitudinal steel under fatigue service load should be limited to 80% of the yield stress. No specific limits were provided for steel stirrups; however, research seems to indicate that the service life of reinforcement is similar whether it is longitudinal or transverse steel (Barnes and Mays 1999).

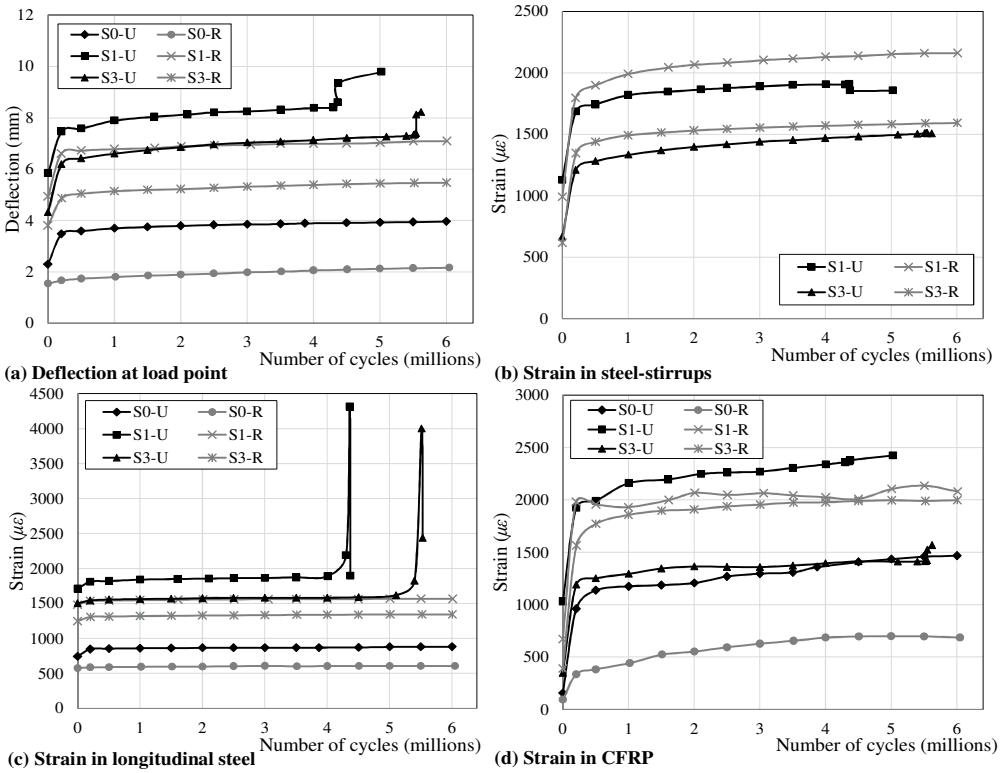


Figure 4. Deflection and strain responses versus number of cycles for $P_{max}$.

### 3.3.2 Longitudinal steel

The strain response in longitudinal steel is illustrated in Figure 4(c). In all specimens and up to failure in some, there was no significant increase in the strains with the increase in number of cycles, and the strain remained quasi-stable during the fatigue loading. However, specimens of category-U with steel stirrups exhibited a sudden increase in strain just before failure. The longitudinal steel yielded at 4.35 and 5.47 million cycles in S1-U and S3-U, respectively.

The longitudinal strains were greater in category-U than category-R specimens due to the extra fatigue loading imposed to upgrade the service load. For both categories, the highest strains were recorded in S1 series; the strain range (and corresponding stress range) at the first cycle was 770 $\mu\varepsilon$ (151 MPa) in S1-U and 680 $\mu\varepsilon$ (133 MPa) in S1-R. As a result, upgrading the service load featured an increase in stress range from 133 to 151 MPa, which resulted in rupture of longitudinal steel. This stress range lies between the upper limits recommended by standards CSA-S6-06 (125 MPa), ACI 215R-74 (138 MPa), and AASHTO LRFD (162 MPa). A similar situation was found with specimens of S3 series, with an increase in stress range from 110 MPa

(560 $\mu\varepsilon$) in S3-R to 133 MPa (680 $\mu\varepsilon$) in S3-U, resulting in rupture of longitudinal steel. This may indicate that code specifications for fatigue limit-state design of unstrengthened RC members may also be used for FRP shear-strengthened structures.

#### 3.3.3 EB-CFRP

The CFRP strains versus number of cycles for all test specimens are illustrated in Figure 4(d). The curves represent the highest strains measured along the shear span. Comparing the S1 and S3 series, it is observed that retrofitted beams featured an enhanced fatigue performance of CFRP with the increase in the amount of transverse steel reinforcement, despite the higher applied loads experienced by S1 specimens. Moreover, in terms of the presence of transverse steel, the specimens with no stirrups (S0 series) exhibited much higher rate of increase in CFRP strain range, and thus more damage accumulation, compared to those with steel stirrups (S1 and S3). This confirms the existence of an interaction and hence of a beneficial stress redistribution between internal shear reinforcement and EB-FRP under fatigue loading.

The maximum strain and strain range in CFRP in both categories were below the maximum threshold values of 0.2 and 0.04% (i.e., corresponding to the first cycle), respectively, as suggested by Czaderski and Motavalli (2004). Moreover, the highest CFRP strain recorded in the last cycle (2430 $\mu\varepsilon$) represented 18% of its ultimate strain (1.33%). The ACI 440.2R-08 guideline states, in this context, that the strain in CFRP for flexural strengthening under fatigue service load should be limited to 55% of its ultimate strength. No specific recommendations were provided for FRP fatigue stress limits with respect to shear strengthening.

### *3.4 Stiffness degradation*

The stiffness measurements of test specimens at each 0.5 million increment fatigue cycles are presented in Figure 5. It is defined as the ratio of the applied load range to the achieved deflection range, corresponding to ($P_{max}$–$P_{min}$). As can be seen, most of the stiffness loss occurred between the first and the 0.5 millionth cycles, followed by a stable region in which the stiffness remained relatively constant until more than 5 million cycles. For category-U specimens that failed in flexure fatigue, an abrupt decrease in stiffness occurred before ultimate failure. It is observed that specimens of category-U exhibited lower stiffness measurements compared to specimens of category-R. For instance, the stiffness in S1-U decreased from 49.79 kN/mm at the first cycle to 42.91 kN/mm at 0.5 million cycles to reach 42.38 kN/mm at 4.35 million cycles (steel yielding) and 38.26 kN/mm at ultimate failure; this represented a total decrease of 23%, where the initial decrease during the first 0.5 million cycles alone was 14%. For comparison, the stiffness of specimen S1-R decreased from 58.13 kN/mm at the first cycle to 45.28 kN/mm at 0.5 million cycles to reach 44.42 kN/mm at 6 million cycles; this represented a stiffness loss of 24%, with 22% in the first 0.5 million cycles.

### *3.5 Static test results subsequent to fatigue loading*

Table 3 summarizes the results from static tests on specimens that did not fail in fatigue. It includes load at rupture $P_n$, total shear resistance $V_n$, as well as shear resistances due to concrete $V_c$, steel $V_s$ and CFRP $V_{frp}$. The presence of transverse steel in retrofitted beams (S0 versus S3 versus S1) resulted in a substantially reduced gain in shear capacity due to CFRP from 76% in specimen S0-R to 23% in S3-R to 19% in S1-R. This confirms the existence of an interaction between steel stirrups and EB-CFRP under static loading, but not yet captured in the guidelines as observed by other researchers since 2002 (Chaallal et al. 2002).

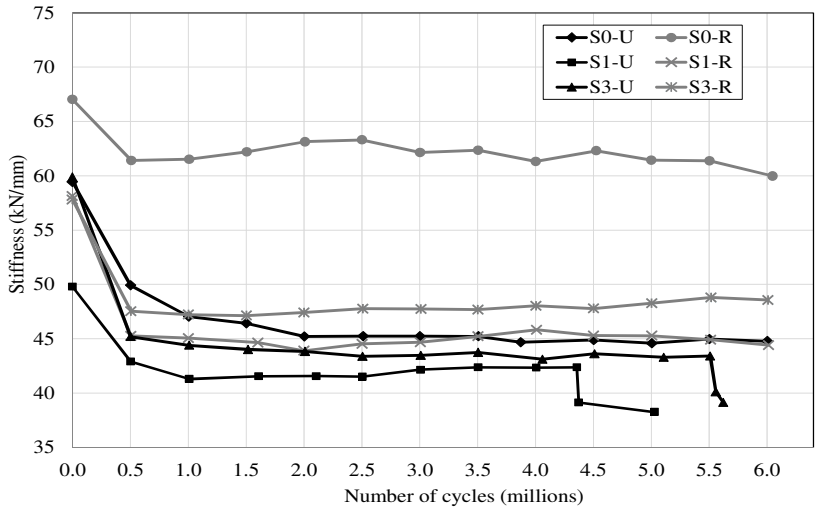


Figure 5. Stiffness at each 0.5 million increment fatigue cycles.

Table 3. Static test results

| | $P_n$ (kN) | $V_n$ (kN) | $V_c$ (kN) | $V_s$ (kN) | $V_{frp}$ (kN) | Gain due to CFRP (%) |
|---|---|---|---|---|---|---|
| S0-U | 209 | 138 | 91 | 0 | 47 | 52 |
| S0-R | 241 | 160 | 91 | 0 | 69 | 76 |
| S1-R | 433 | 287 | 91 | 151 | 45 | 19 |
| S3-R | 362 | 240 | 91 | 104 | 45 | 23 |

## 4 CONCLUSIONS

The following conclusions can be drawn:

- All specimens exhibited a typical trend of cumulative fatigue degradation, characterized by an accelerated rate of damage propagation during the early cycles, followed by a stable phase in which the damage accumulation slowed significantly;
- In RC beams shear strengthened with CFRP sheets to upgrade the service load, the longitudinal steel may be the weakest link and should be looked at with caution, especially for extended service life, where it may govern the upper limit of the projected capacity;
- The retrofitted specimens featured an enhanced fatigue performance of CFRP with the increase in the amount of transverse steel reinforcement, confirming thereby the existence of an interaction between steel-stirrups and EB-FRP.

## 5 REFERENCES

AASHTO. 2010. “AASHTO LRFD Bridge Design Specifications, 5th Edition”. *American Association of State Highway and Transportation Officials (AASHTO)*, Washington, DC.

ACI 215R-74. Revised 1992/Reapproved 1997. “Considerations for design of concrete structures subjected to fatigue loading”. *American Concrete Institute (ACI) Committee 215*, Farmington Hills, Michigan.

ACI 440.2R-08. 2008. "Guide for the design and construction of externally bonded FRP systems for strengthening concrete structures". *American Concrete Institute (ACI) Committee 440*, Farmington Hills, Michigan.

Bae, SW, Murphy, M, Mirmiran, A, and Belarbi, A. 2013. "Behavior of RC T-Beams Strengthened in Shear with CFRP under Cyclic Loading". *Journal of Bridge Engineering,* 18(2): 99-109.

Barnes, RA, and Mays, GC. 1999. "Fatigue Performance of Concrete Beams Strengthened with CFRP Plates". *Journal of Composites for Construction,* 3(2): 63-72.

Chaallal, O, Boussaha, F, and Bousselham, A. 2010. "Fatigue Performance of RC Beams Strengthened in Shear with CFRP Fabrics". *Journal of Composites for Construction,* 14(4): 415-423.

Chaallal, O, Shahawy, M, and Hassan, M. 2002. "Performance of reinforced concrete T-girders strengthened in shear with carbon fiber-reinforced polymer fabric". *ACI Structural Journal,* 99(3): 335-343.

CSA-S6-06. 2006. "Canadian Highway Bridge Design Code". *Canadian Standards Association (CSA) Committee S6*, Mississauga, Ontario.

Czaderski, C, and Motavalli, M. 2004. "Fatigue behaviour of CFRP L-shaped plates for shear strengthening of RC T-beams". *Composites Part B: Engineering,* 35(4): 279-290.

Williams, G, and Higgins, C. 2008. "Fatigue of Diagonally Cracked RC Girders Repaired with CFRP". *Journal of Bridge Engineering,* 13(1): 24-33.